World Academy of Science, Engineering and Technology
International Journal of Mechanical and Mechatronics Engineering
Vol:9, No:8, 2015

Influence of Flame-Holder on Existence Important Parameters in a Duct Combustion Simulator

M. M. Doustdar, M. Mojtahedpoor

***Abstract*—**The effects of flame-holder position, the ratio of flame holder diameter to combustion chamber diameter and injection angle on fuel propulsive droplets sizing and effective mass fraction have been studied by a cold flow. We named the mass of fuel vapor inside the flammability limit as the effective mass fraction. An empty cylinder as well as a flame-holder which are a simulator for duct combustion has been considered. The airflow comes into the cylinder from one side and injection operation will be done by four nozzles which are located on the entrance of cylinder. To fulfill the calculations a modified version of KIVA-3V code which is a transient, three-dimensional, multiphase, multi component code for the analysis of chemically reacting flows with sprays, is used.

***Keywords*—**KIVA-3V, flame-holder, duct combustion, effective mass fraction, mean diameter of droplets.

I. Introduction

DROPLET sizing has relevance to many practical combustion devices, including, Diesel, and gas turbine engines, as well as oil-fired boilers, furnaces, and process heaters. In these devices, spray combustion is the dominant feature. The problem of droplet burning includes both the evaporation and the combustion process. Solving problems concerning droplet evaporation and combustion needs the use of mass transfer and thermodynamic laws and equations. In all the above systems, liquid fuels and/or oxidizer are usually injected into the combustion chamber as a spray of droplets. Research on the gasification, oxidation, and dynamics of fuel droplet commands both practical and fundamental interest to energy and combustion science. According to law, droplet combustion is a problem involving complex chemically reacting multi component two-phase flows with phase change, rich in physical and chemical phenomena typically to be studied.

Liquid fuel spray combustion involves different complicated and inter-related processes such as atomization, subsequent droplet breakup and collisions, vaporization, fuel vapor-air mixing, and finally chemical reactions. Understanding these processes and being able to represent them in the context of a CFD simulation program are of great importance both for researchers and for the industry. CFD offers a significant and a powerful tool to evaluate the operation of practical combustion systems and helps designers of these systems to come up with modified versions that have better performance characteristics.

Mohammad Mahdi Doustdar is with the Imam Hossein University, (e-mail: mmdoustdar@yahoo.com).

Mohammad Mojtahedpoor is with the Malek-e-Ashtar University of Technology.

The researches, which focus on the fuel/air mixing phenomena or reactive flows, are very rare in open literatures either by using numerical methods [1]-[4]. As some new researches in this field, the effects of injection angle, length-to-diameter, entrance airflow velocity and injection velocity on droplets sizing have been done by [5]-[9].

In the present study, the influence of flame-holder position and the ratio of flame-holder diameter to combustion chamber diameter on fuel propulsive droplets sizing and effective mass fraction have been numerically investigated as well as the effect of flame-holder on flow fields is shown.

II. Numerical Modeling

The computer program, used in this work is a KIVA-3V based code. The numerical procedure used in this simulation is based on the discrete-droplet model (DDM). In this model, the entire spray is represented by finite numbers of groups of particles. Each particle represents a number of droplets of identical size, velocity and temperature. A Lagrangian formulation is used to track the motion and transport of particles through the flow field and an Eulerian formulation is used to solve the governing equations for the gas phase. The gas phase solution procedure is based on the ALE (Arbitrary Lagrangian-Eulerian) finite volume method. Implicit differencing is used for the terms associated with pressure wave propagation and for all the diffusion terms. Explicit differencing is used to calculate convection terms.

To avoid the restriction of time step by the courant stability condition, the convection calculation is sub cycled. The turbulent law of the wall is employed to calculate wall heat transfer and boundary layer drag. We have used a standard version of the k-ε turbulence model. The effects of droplets on the gas phase are considered by designating proper source terms in the gas phase conservation equations. The particles and gas interact by exchanging mass, momentum and energy. For assigning droplet properties at injection or anywhere in downstream, a probability concept is applied. A Monte Carlo sampling technique is used to calculate droplet properties. More description is well documented in [10].

III. Governing Equations

A spherical droplet of pure liquid, initially at temperature T_0 and radius R_0 is suddenly subjected to surrounding gas at uniform temperature T_e. The only convective motion considered is that induced by the evaporation process itself, giving rise to a radial convective velocity in the vapor (species

1) and gas (species 2) mixture. The governing conservation equations are:

1. Liquid Phase, $r < R(t)$

(A) Energy

$$\frac{\partial T}{\partial t} = \alpha_l \frac{1}{r^2}\frac{\partial}{\partial r}\left(r^2 \frac{\partial T}{\partial r}\right). \quad (1)$$

2. Vapor Phase, $r > R(t)$

(A) Mass

$$\frac{\partial \rho}{\partial t} + \frac{1}{r^2}\frac{\partial}{\partial r}(\rho r^2 \upsilon_r) = 0. \quad (2)$$

(B) Momentum

$$\frac{\partial \upsilon_r}{\partial t} + \upsilon_r \frac{\partial \upsilon_r}{\partial r} = \frac{1}{\rho r^2}\frac{\partial}{\partial r}\left(\frac{4}{3}\mu r^2 \frac{\partial \upsilon_r}{\partial r}\right) - \frac{8}{3}\frac{\mu}{\rho}\frac{\upsilon_r}{r^2} - \frac{4}{3}\frac{\upsilon_r}{\rho r}\frac{\partial \mu}{\partial r} - \frac{1}{\rho}\frac{\partial P}{\partial r}. \quad (3)$$

(C) Species

$$\frac{\partial m_1}{\partial t} + \upsilon_r \frac{\partial m_1}{\partial r} = \frac{1}{\rho r^2}\frac{\partial}{\partial r}\left(\frac{\mu}{Sc} r^2 \frac{\partial m_1}{\partial r}\right). \quad (4)$$

(D) Energy

$$\frac{\partial T}{\partial t} + \upsilon_r \frac{\partial T}{\partial r} = \frac{1}{\rho r^2}\frac{\partial}{\partial r}\left(\frac{\mu}{\Pr} r^2 \frac{\partial T}{\partial r}\right) + \frac{\wp_{12}}{C_p}\frac{\partial T}{\partial r} \times \left[\left(C_{p1} - C_{p2}\right)\frac{\partial m_1}{\partial r} + \frac{Sc}{\Pr}\frac{\partial C_p}{\partial r}\right]. \quad (5)$$

The boundary conditions and constants are:

1. Liquid Phase, at $r = 0$

$$r = 0 \quad (6)$$

2. Vapor Phase, as $r \to \infty$

$$m_1 \to 0; T \to T_e; \upsilon_r \to 0; P \to P_e. \quad (7)$$

3. At the Interface, $r = R$

$$\upsilon_r = \dot{m}''\left(\frac{1}{\rho} - \frac{1}{\rho_l}\right) \quad (8)$$

$$\left(1 - m_{1,s}\right)\dot{m}'' = -\rho \wp_{12} \left.\frac{\partial m_1}{\partial r}\right|_s \quad (9)$$

$$T_s = T_u \quad (10)$$

$$k \left.\frac{\partial T}{\partial r}\right|_s = k \left.\frac{\partial T}{\partial r}\right|_u + \dot{m}'' \hat{h}_{fg} \quad (11)$$

$$\frac{dR}{dt} = -\frac{\dot{m}''}{\rho_l} \quad (12)$$

$$m_{1,s} = m_{1,s}(P, T_s). \quad (13)$$

In addition, there is an equation of state; assuming ideal gas mixture, P=ρRT/M. Initial conditions for the problem are, in a practical sense, somewhat arbitrary. The approach adopted here is discussed below along with other numerical procedures. Additional assumptions include (i) constant liquid phase properties, (ii) no second order diffusion effects, and (iii) thermodynamic equilibrium at the interface. Furthermore, the variable property calculations showed that P deviated from *P*, by less than 0.3 percent; thus, *P* = *P* was assumed for the reference property analysis, making equation (3) irrelevant where P is ambient pressure.

IV. Mesh Generation

The KIVA-3 formulation is based on (x, y, z) Cartesian coordinates. Rather than being confined to one logical block of cells in (i, j, k) space to encompass the entire region to be modeled, however, the geometry of a KIVA-3 mesh is composed of any arbitrary number of logical blocks that are patched together in a completely seamless fashion. Patching allows complex geometries to be created block by block, while minimizing the number of deactivated zones. In fact, the only deactivated zones are the ghosts that surround the final mesh, as there are no ghosts between blocks where common faces are joined. The ghosts enable the application of boundary conditions at inflow/outflow cell faces, as they provide logically situated outside storage for fluxed quantities.

With regard to the injection initial conditions, the dimensions of the computation domain are selected. As the injection velocity, or fuel total mass, increases, a larger domain of computation should be considered. Illustrated five mesh types, which would be a possible block type in the K3PREP grid generator, are shown in Fig. 1.

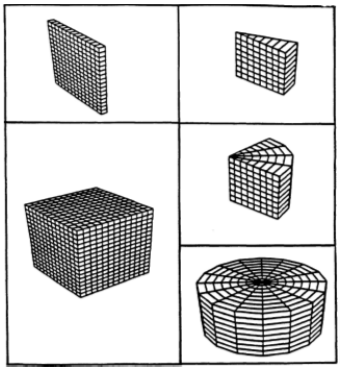

Fig. 1 K3PREP building meshes or portions of meshes using these five generic block shapes

In accordance with mesh generation descriptions, the considered mesh of this study has been shown in Fig. 2.

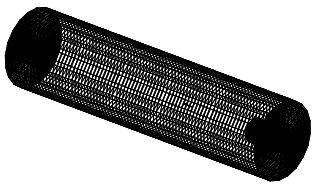

Fig. 2 The sample mesh

V. Boundary Conditions

In this study we have considered a cylinder with a flame-holder. The air comes into the cylinder from one side and after mixing with injected fuel, exhausted at the end of combustor. The length of this cylinder is 40cm and the diameter is 10cm. The distance of flame-holder from entrance airflow is changed from 4 to 7, 10 and finally 12cm. Also, by changing the ratio of flame-holder diameter to combustion chamber diameter from 18 to 20, 26, 28, 30 and 40 percent, the mean diameter of

droplets sizing and effective mass fraction have been investigated. The specification of mentioned mesh has been shown in Fig. 3 and a perspective view of this simulated combustor model is illustrated in Fig. 4.

Fig. 3 Geometry and dimension of the simulated combustor model

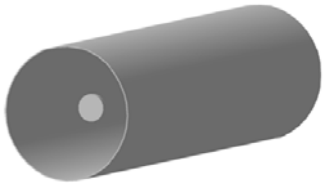

Fig. 4 Perspective view of simulated combustor model

As the boundary conditions, "pressure inflow" for entrance area and equal 1 atm, "pressure outflow" for exit area have been considered. The boundary condition of walls has been considered "solid" also. A complete format of initial conditions has been exhibited in Table I.

TABLE I
INITIAL CONDITIONS

	Fuel Droplets	Air Flow
Total fuel mass flow	20 g/s	------
Temperature	300 K	300 K
Velocity	30 m/s	26 m/s
Initial Sauter radius	0.01 cm	------
Injection angle	90° (cross flow)	------

VI. Solving Pattern

The time of solving has considered 1 second and the time of fuel injection is 0.02 second after solving beginning in due to the fact that the flow in cylinder becomes pervasive. All of calculations have been done by KIVA-3V code modified for this purpose.

VII. Results and Discussion

A. The Role of Flame Holder

A flame holder is a component of a jet engine designed to help maintain continual combustion. All continuous-combustion jet engines require a flame holder. A flame holder creates a low-speed eddy in the engine to prevent the flame from being blown out. The design of the flame holder is an issue of balance between a stable eddy and drag. The produced vortices after the flame-holder are shown in Fig. 5.

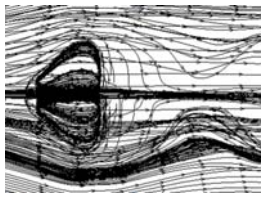

Fig. 5 The produced vortices after flame-holder

B. d/D Ratio

In the first step, we have studied about the ratio of flame-holder's diameter (d) to combustor's diameter (D). For this purpose, we have considered an empty cylinder plus a flame-holder with diameter ratio of 18 percent and the mean diameter of propulsive droplets sizing and effective mass fraction have been investigated. Then, by increase of this ratio from 18 to 20, 26, 28, 30 and finally 40 percent, these computations are repeated. The results of these calculations have been illustrated in Table II.

TABLE II
THE MEAN DIAMETER AND EFFECTIVE MASS FRACTION IN DIFFERENT I

Parameters	d/D ratio					
	18	20	26	28	30	40
Mean diameter(μm)	0.63	0.43	0.5	0.42	0.49	0.51
Mean efficient mass fraction(percent)	96.1	98.2	97.7	96.3	95.8	64

According to Table II, by growth of d/D ratio from 18 to 20 percent, the mean diameter of fuel droplets sizing has decreased. Then, with rise of this ratio from 20 to 26, 28, 30 and 40 percent respectively, however the mean diameter has some fluctuations, but it is approximately constant. The gotten graph has been shown in Fig. 6.

In accordance with Fig. 6 and initial conditions, the ratio of flame-holder's diameter (d) to combustor's diameter (D) do not influence on mean diameter of droplets so much. However the smallest droplets have been appeared in d/D percentages of 20 and 28.

About the effective mass fraction, at first, by increasing the d/D ratio from 18 to 20, the effective mass fraction has risen. Then, with growth of this ratio from 20 to 26, 28 and 30 percent correspondingly, the effective mass fraction has fallen gradually, but with raise of this percentage from 30 to 40, the effective mass fraction has decreased sharply. The variation of effective mass fraction in different ratios has been exhibited in Fig. 7.

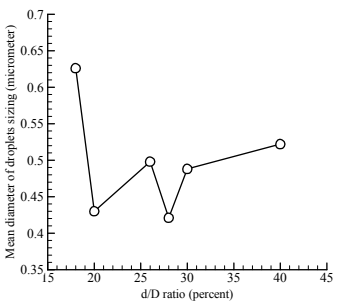

Fig. 6 The variation of mean diameter in different d/D ratios

In agreement with Fig. 7, the most amount of effective mass fraction has been appeared in d/D ratio of 20 percent. Also, at d/D ratio of 40 percent, the effective mass fraction has dropped dramatically; it seems this manner is because of the high amount of blockage. In next, we consider the d/D ratio as 20 percent.

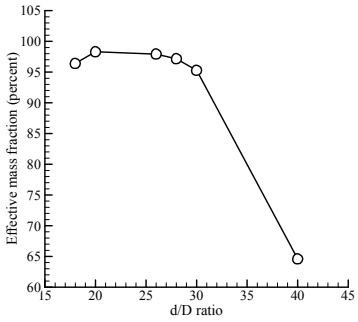

Fig. 7 The fluctuation of effective mass fraction in different ratios

C. Flame Holder Position and Injection Angle

In this part, we are looking for a good position for the flame-holder as well as the best injection angle. For this purpose, we have changed the position of flame-holder from 4cm after entrance area to 7, 10 and finally 12 cm. Also, we have repeated this investigation for different injection angles. In Table III, the initial conditions for this study have been shown.

TABLE III
INITIAL CONDITIONS

	Fuel Droplets	Air Flow
Total fuel mass flow	20 g/s	------
Temperature	300 k	300 k
Velocity	30 m/s	26 m/s
Initial Sauter radius	0.01 cm	------
d/D Ratio	20 (percent)	------

The fuel has been injected in different injection angles. At first, we injected the fuel at injection angle of 0^o and it means injection at flow direction. Then we have increased this angle from 0^o to 30^o, 45^o, 60^o, 90^o and finally 120 degree. The injection at injection angle of 90^o is cross flow and the injection angle of 120^o is counter flow injection. The results of these computations have been shown in Figs. 8 and 9.

In accordance with Fig. 8, with increase of injection angle from 0^o to 30^o, the mean diameter of droplets sizing has fallen suddenly. Then, by growth of injection angle to 45^o, 60^o, 90^o and finally 120 degree respectively, the mean diameter has had some fluctuations but these variations were not so much.

Also in Fig. 9, we have ignored the injection angle of 0^o, and the mean diameter of droplets sizing has been shown in details. According to Fig. 9, however in all different distances from entrance area the mean diameters do not have so much variation, but in all of distances the least droplets have been appeared at injection angles of 60^o and 90 degree.

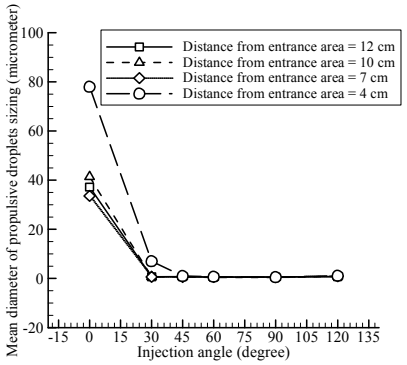

Fig. 8 The fluctuations of mean diameter in different injection angles

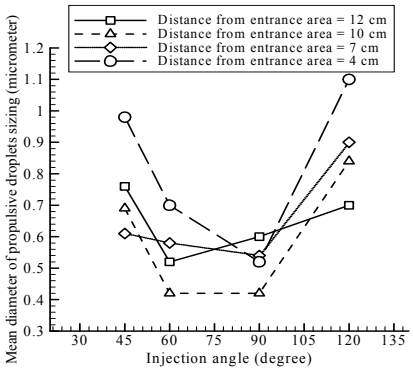

Fig. 9 The fluctuations of mean diameter in different injection angles

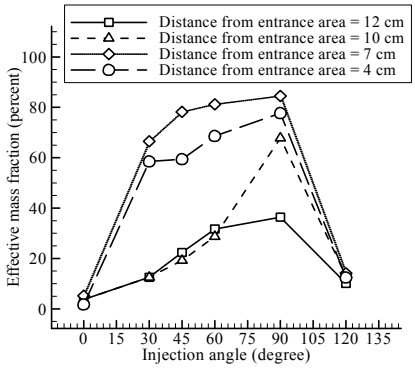

Fig. 10 The variation of effective mass fraction in different injection angles

Fig. 10 shows the effects of injection angle on effective mass fraction. In accordance with Fig. 10, by growth of injection angle from 0^o to 30^o, the effective mass fraction has risen sharply, and then with increase of this angle to 45^o up to 90^o (cross flow) the effective mass fraction has increased gradually, but at injection angle of 120^o, this quantity has dropped dramatically. In accordance with Fig. 10, in all cases; the maximum quantities of effective mass fraction have been appeared at injection angle of 90 degree, so it can be considered as an optimum angle in injection.

D.The Position of Flame-Holder and Effective Mass

In this part, the effect of flame-holder position on effective mass fraction has been investigated. The obtained results of this calculation have been illustrated in Fig. 11.

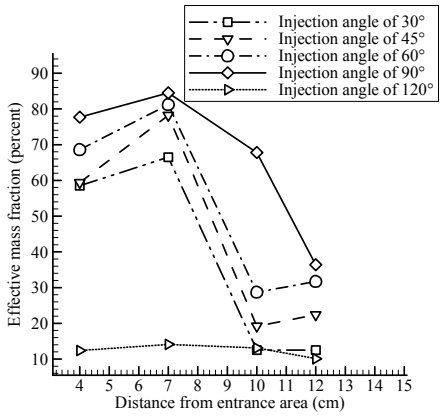

Fig. 11 The fluctuations of effective mass fraction in different distances of flame-holder

According to Fig. 11, with increase of distance from 4 to 7cm the effective mass fraction has risen sharply, then by increasing this distance to 10cm the effective mass fraction has fallen dramatically. So it seems the most quantities of effective mass fraction have been appeared at distance area of 7cm.

VIII. Conclusion

The effects of flame holder position and injection angle on effective mass fraction and propulsive droplets sizing have been investigated by a numerical procedure.

The results show, in different injection angles, the most quantity of effective mass fraction has been appeared at the respect of flame-holder's diameter to combustor's diameter of 20 percent. Also in this ratio, the mean diameter of propulsive droplets sizing is lesser than other respects.

The consequences show, by growth of injection angle from inflow direction to counter flow direction, the mean diameter of droplets decreases till cross flow injection and then increases and the least amounts of this parameter appear at injection angle of 60^o and 90 degree also.

With increase of injection angle, the effective mass fraction increases gradually until cross flow and then decreases. The maximum of effective mass fraction appears at injection angle of 90 degree. It seems in accordance with our initial conditions and results, the injection angle of 90^o is the best angle for our case.

The results show, in different flame holder positions, the maximum of effective mass fraction appears in distance from entrance area of 7 cm.

References

[1] S. R. Turns, (2000), "*An introduction to Combustion Concepts and Applications*", Second edition, Chapter 10, pp. 369–410.

[2] G. L Hubbard, Denny V. E. and Mills, A. F. (1975), "*Droplet evaporation: Effects of transients and variable properties*," International Journal of Heat and Mass Transfer, 18(9), pp. 1003-1008.

[3] F. R. Newbold, and Amundson, N. R. (1973), "A model for evaporation of a multi-component droplet," AIChE journal,19(1),pp. 22-30B. Smith, "An approach to graphs of linear forms (Unpublished work style)," unpublished.

[4] K. Prommersberger, Maier G. and Wittig S.(1998) "Validation and Application of a Droplet Evaporation Model for Real Aviation Fuel," RTO AVT Symposium on Gas Turbine Combustion, Emissions and Alternative Fuels, TO-MP-14, pp. 16.1- 16.12.

[5] M. M. Doustdar, Mojtahedpoor, M. (2011), "A Numerical Study of the Effect of Pressure on Propulsive Droplets Sizing in a Duct by KIVA-3V Code," Applied Mechanics and Materials Journal, 110-116, pp. 4527-4531.

[6] M. M. Doustdar, Mojtahedpoor, M. (2011), "The Effects of Fuel Injection Angle and Injection Velocity on Propulsive Droplets Sizing in a Duct," Applied Mechanics and Materials Journal, 110-116, pp. 2879-2887.

[7] M. Mojtahedpoor, Doustdar, M. M. (2011), "A Numerical Study on the Effects of Injection Spray Cone and Pressure on Propulsive Droplets in a Ramjet," World Academy of Science, Engineering and Technology Journal, 5, pp. 163-167.

[8] M. M. Doustdar, Mojtahedpoor, M. (2011), "Effects of Injection Velocity and Entrance Air Flow Velocity on Droplet Sizing in a Duct," World Academy of Science, Engineering and Technology journal, 5, pp. 814-817.

[9] M. M. Doustdar, Mojtahedpoor, M., Wadizadeh, M. (2011) "Effects of Injection Initial Conditions and Length-to-Diameter Ratio on Fuel Propulsive Droplets Sizing in a Duct," Applied Mechanics and Materials Journal, 110-116, pp. 1784-1792.

[10] A. Amsden, O'Rourke, P. J. and Butler T. D. (1989) "*KIVA-II: A Computer Program for Chemically Reactive Flows with Sprays*," Los Alamos National Laboratory Report, LA-11560-MS.